Available online at www.sciencedirect.com
ScienceDirect
Trans. Nonferrous Met. Soc. China 29(2019) 25−33
Transactions of Nonferrous Metals Society of China
www.tnmsc.cn

Experimental determination of 800 °C isothermal section in Al−Zn−Zr ternary system

Yong-xiong LIU[1,2], Fu-cheng YIN[1,2], Zhi LI[1,2], Xue-mei OUYANG[1,2], Liang-ping CHEN[1,2]

1. School of Materials Science and Engineering, Xiangtan University, Xiangtan 411105, China;
2. Key Laboratory of Materials Design and Preparation Technology of Hunan Province, Xiangtan University, Xiangtan 411105, China

Received 25 September 2017; accepted 12 March 2018

Abstract: The 800 °C isothermal section in the Al−Zn−Zr system was investigated using the equilibrated alloy method and the solid/liquid diffusion couple approach by means of scanning electron microscopy equipped with energy dispersive spectroscopy, X-ray powder diffraction and electron probe microanalysis. Thirteen three-phase regions are experimentally confirmed in the ternary system. A ternary compound $Zn_{50}Al_{25}Zr_{25}$ named as *T* phase exists stably in the 800 °C isothermal section. Its composition range varies widely (16.84−55.1 at.% Zn, 18.02−56.3 at.% Al and 26.0−28.53 at.% Zr), and it can be in equilibrium with all the binary compounds. The maximum solubilities of Zn in Zr_3Al, Zr_2Al, Zr_3Al_2, Zr_4Al_3, ZrAl, Zr_2Al_3, $ZrAl_2$ and $ZrAl_3$ are 7.5, 0.84, 0.33, 0.89, 0.91, 1.12, 0.64 and 3.8 at.%, respectively. The maximum solubilities of Al in Zn_3Zr, Zn_2Zr and ZnZr are 1.6, 1.3 and 13.6 at.%, respectively.

Key words: Al−Zn−Zr system; phase diagram; $Zn_{50}Al_{25}Zr_{25}$; SEM−EDS; EPMA

1 Introduction

Aluminum−zinc-based alloys have been broadly applied to the aerospace and automotive manufacturing industries owing to their high specific strength and good stress corrosion resistance [1,2]. Micro-alloying is an important modification technology for metal materials and has been widely used in the aluminum−zinc-based alloys to further improve their overall performance [3−5]. The transition metal Zr is an effective alloying element [6−10], and its addition can enhance the formation of the dispersoid Al_3Zr, which inhibits the recrystallization process and hence refines the grain size [11]. The effects of Zr concentration and homogenization temperature on the formation of the Al_3Zr dispersoid and the recrystallization behavior have been extensively studied [12−14]. The Zr addition into the aluminum−zinc-based alloys increases the density of the dispersoid, while the homogenization temperature mainly influences the size, number and distribution of the dispersoid. Knowledge of phase equilibrium in the Al−Zn−Zr ternary system is useful to fully understand the effect of Zr on the recrystallization process.

Besides, the element Zr has often been added into the Zn−Al baths to improve the microstructure of the hot-dipped coating. It was reported that the Zr addition induced the forming of a ternary compound in the Zn coating and hence controlled the Zn−Fe reaction in the Si-contained steels, decreasing the coating thickness in general galvanizing [15,16]. Therefore, in order to optimize the aluminum−zinc-based alloys and Zn−Al hot-dipped coating, it is important to obtain the phase equilibria of the Al−Zn−Zr ternary system. The 450 °C isothermal section of the Al−Zn−Zr system has been experimentally determined by CHEN et al [17]. In order to get more phase equilibria and enough data for thermodynamic assessment about the Al−Zn−Zr system, the isothermal section at 800 °C in the Al−Zn−Zr ternary system has been investigated experimentally in the present work.

In the Al−Zn−Zr ternary system, the constituent binary phase diagrams of Al−Zn [18−20], Zn−Zr [21−23] and Al−Zr [24,25] have been investigated. The information about these binary phase diagrams has been summarized in Ref. [17]. A ternary compound Al_3ZnZr_2

Foundation item: Projects (51771160, 51471140) supported by the National Natural Science Foundation of China
Corresponding author: Fu-cheng YIN; Tel: +86-731-58298428; E-mail: fuchengyin@xtu.edu.cn, lizhiclsj@xtu.edu.cn
DOI: 10.1016/S1003-6326(18)64911-8

was found in the Al−Zn−Zr ternary system at 800 °C by DRASNER and BLAZINA [26], while it was not confirmed at 450 °C. Another ternary compound $Zn_{50}Al_{25}Zr_{25}$ was reported [17] and its structure was identified as Cu_3Au-type by SCHUBERT et al [27]. The crystallographic data of the binary compounds in the Al−Zn−Zr system are listed in Table 1. The phase boundaries of the isothermal section of the Al−Zn−Zr ternary system in this work are constructed based on the three binary phase diagrams [20,21,24].

2 Experimental

Due to the high liquidus temperature of the Al−Zr compounds, the diffusion couple method was used to investigate the phase equilibria of the Al−Zn−Zr ternary system at the Al−Zr side. Seven Al−Zr binary alloys $Zr_{29}Al_{71}$, $Zr_{36}Al_{64}$, $Zr_{45}Al_{55}$, $Zr_{53}Al_{47}$, $Zr_{58}Al_{42}$, $Zr_{64}Al_{36}$ and $Zr_{71}Al_{29}$, containing two different Al−Zr compounds at 800 °C, were prepared by melting Al ingots and Zr chips in an arc-furnace with a nonconsumable tungsten electrode under high purity argon atmosphere. The purity of the raw materials was 99.99%. Slices of approximate 6 mm × 6 mm × 4 mm were cut by wire-electrode from these Al−Zr alloys. Each sample was polished, cleaned, dried and then sealed together with 16 g zinc ingot under argon atmosphere in a vacuumized quartz tube. The sealed samples were kept at 800 °C for 6 h, and then quenched into water quickly.

The phase relationships of the Al−Zn−Zr system were investigated by the equilibrated alloys. The purity of the raw materials was 99.99%. For each alloy, the total mass of the three raw materials is 3 g, with an accuracy of 0.0001 g. Because Al can react with SiO_2 at elevated temperature, the three raw materials were mixed and put into an Al_2O_3 crucible and then were sealed in a vacuumized quartz tube. Each sample was heated to 1150 °C for 24 h, and then quenched into water quickly with bottom quenching technique [34] to reduce the Zn loss. Each quenched sample was resealed in quartz tube with a corundum crucible and annealed at 800 °C for 15 d. After annealing, all samples were immediately quenched into water to preserve the equilibrated state at 800 °C.

The final sample was cut into two parts. One part was used for micro-structural examination. Detailed metallographic examinations and compositional analyses of all phases in the samples were investigated using a JSM−6360LV SEM equipped with an OXFORD INCA EDS under BES mode. The other one was prepared to further confirm the phase constitution by analyzing XRD, operating at 40 kV and 40 mA with Cu K_α radiation. The chemical compositions of the reaction zone in the diffusion couples were determined by EPMA (JEOL JXA−8230) operating at 15 kV. Pure elements Al, Zn and Zr standards provided by JEOL were used for calibration.

3 Results and discussion

3.1 Diffusion couples

The use of diffusion couples in phase diagram studies is based on the principle of local equilibria at the phase interfaces in the diffusion zone [35]. A total of seven diffusion couples (DCs) were prepared in this work. The compositions of three phases of each tie-triangle in the local equilibria obtained by EPMA from these seven DCs are listed in Table 2.

The microstructure of the representational DC $Zr_{64}Al_{36}$/Zn annealed at 800 °C for 6 h is shown in Fig. 1(a). It can be seen that the diffusion path of the DC $Zr_{64}Al_{36}$/Zn is $Zr_3Al_2 + Zr_2Al \rightarrow Zr_3Al_2 + T \rightarrow Zr_2Al + T \rightarrow T + Zn_3Zr \rightarrow Zn_3Zr + L\text{-}Zn \rightarrow L\text{-}Zn$. Five phases Zr_3Al_2, Zr_2Al, T, Zn_3Zr and L-Zn are confirmed by XRD

Table 1 Crystallographic data of binary compounds in Al−Zn−Zr system

Phase	Pearson symbol	Space group	Prototype	Lattice parameter/nm			Ref.
				a	*b*	*c*	
Zr_3Al	*cP*4	$Pm\bar{3}m$	Cu_3Au	0.4380	0.4380	0.4380	[28]
Zr_2Al	*hP*6	*P*63/*mmc*	NiIn	0.4894	−	0.5928	[29]
Zr_3Al_2	*tP*20	*P*42/*mnm*	Zr_3Al_2	0.7630	0.7630	0.6990	[28]
Zr_4Al_3	*hP*7	$P\bar{6}$	Zr_4Al_3	0.5386	0.5430	0.5430	[28]
ZrAl	*oC*8	*Cmcm*	CrB	0.3353	1.0866	0.4266	[29]
Zr_2Al_3	*oF*40	*Fdd*2	Zr_2Al_3	0.5549	0.5549	0.7490	[28]
$ZrAl_2$	*hP*12	*P*63/*mmc*	$MgZn_2$	0.5301	0.5301	0.8760	[30]
$ZrAl_3$	*tI*16	*I*4/*mmm*	$ZrAl_3$	0.3999	0.3999	1.7283	[31]
ZnZr	*cP*2	$Pm\bar{3}m$	CsCl	0.3336	0.3336	0.3336	[32]
Zn_2Zr	*cF*24	$Fd\bar{3}mS$	$MgCu_2$	0.5230	0.5230	0.5230	[33]
Zn_3Zr	*cP*2	$Pm\bar{3}m$	$TiZn_3$	0.8160	0.8160	0.7957	[32]

Table 2 Tie-triangle data obtained with EMPA analyses for diffusion couples at 800 °C

Diffusion couple	Tie-triangle	Phase	Composition/at.%		
			Zn	Al	Zr
$Zr_{71}Al_{29}$/Zn	Zr_3Al+Zr_2Al+*T*	Zr_3Al	1.55	23.47	74.98
		Zr_2Al	0.84	31.45	67.71
		T	53.16	18.76	28.08
	T+ Zn_3Zr+*L*-Zn	Zn_3Zr	71.38	0.17	28.45
		T	53.71	18.73	27.56
		L-Zn	95.23	0.02	4.75
$Zr_{64}Al_{36}$/Zn	Zr_2Al+Zr_3Al_2+*T*	Zr_2Al	0.27	32.86	66.87
		Zr_3Al_2	0.25	39.98	59.77
		T	53.45	18.02	28.53
	T+Zn_3Zr+*L*-Zn	Zn_3Zr	72.57	1.24	26.19
		T	54.35	18.12	27.53
		L-Zn	94.01	0.84	5.15
$Zr_{58}Al_{42}$/Zn	Zr_3Al_2+Zr_4Al_3+*T*	Zr_3Al_2	0.33	40.20	59.47
		Zr_4Al_3	0.82	41.93	57.25
		T	48.88	24.32	26.80
	T+Zn_3Zr+*L*-Zn	Zn_3Zr	72.35	1.48	26.17
		T	53.41	18.04	28.55
		L-Zn	84.39	1.58	14.03
$Zr_{53}Al_{47}$/Zn	Zr_4Al_3+ZrAl+*T*	Zr_4Al_3	0.89	41.58	57.53
		ZrAl	1.12	48.63	50.25
		T	51.27	20.72	28.01
	T+Zn_3Zr+*L*-Zn	*T*	52.43	21.11	26.46
		Zn_3Zr	72.57	1.60	25.83
		L-Zn	89.35	0.78	9.87
$Zr_{45}Al_{55}$/Zn	ZrAl+Zr_2Al_3+*T*	ZrAl	0.69	49.53	49.78
		Zr_2Al_3	0.91	55.78	43.31
		T	35.67	36.12	28.21
	T+Zn_3Zr+*L*-Zn	*L*-Zn	79.86	11.23	8.91
		Zn_3Zr	72.31	1.10	26.59
		T	36.85	35.79	27.36
$Zr_{36}Al_{64}$/Zn	Zr_2Al_3+$ZrAl_2$+*T*	Zr_2Al_3	0.53	56.03	43.44
		$ZrAl_2$	0.53	62.83	36.64
		T	29.18	43.34	27.48
	T+Zn_3Zr+*L*-Zn	*T*	35.16	38.66	26.18
		Zn_3Zr	72.34	1.49	26.17
		L-Zn	99.09	0.73	0.18
$Zr_{29}Al_{71}$/Zn	$ZrAl_2$+*T*+$ZrAl_3$	$ZrAl_2$	0.64	63.03	36.33
		T	16.84	55.74	27.42
		$ZrAl_3$	0.24	71.92	27.84
	T+Zn_3Zr+*L*-Zn	*T*	29.45	43.62	26.93
		Zn_3Zr	72.39	1.58	26.03
		L-Zn	99.27	0.50	0.23

patterns shown in Fig. 1(b). The ternary compound $Zn_{50}Al_{25}Zr_{25}$ is marked as *T* in the present work, which was reported by SCHUBERT et al [27] and confirmed at 450 °C by CHEN et al [17]. However, another ternary compound Al_3ZnZr_2 is not found in this work. In the diffusion couples, the zinc-rich solid solution phase is marked as *L*-Zn in this work because it is in liquid state at 800 °C. There are (Zr_3Al_2+Zr_2Al+*T*) and (*T*+Zn_3Zr+*L*-Zn) three-phase local equilibria at the conjunction interface. From Table 2, it can be seen that the

compositions of these three phases in the same tie-triangle determined from different DCs are similar. So, the diffusion couple method in phase diagram studies is reliable and efficient.

For the other six DCs $Zr_{71}Al_{29}$/Zn, $Zr_{58}Al_{42}$/Zn, $Zr_{53}Al_{47}$/Zn, $Zr_{45}Al_{55}$/Zn, $Zr_{36}Al_{64}$/Zn and $Zr_{29}Al_{71}$/Zn, their diffusion paths are indicated in Fig. 2. Each of them has the analogical diffusion path as the DC $Zr_{64}Al_{36}$/Zn.

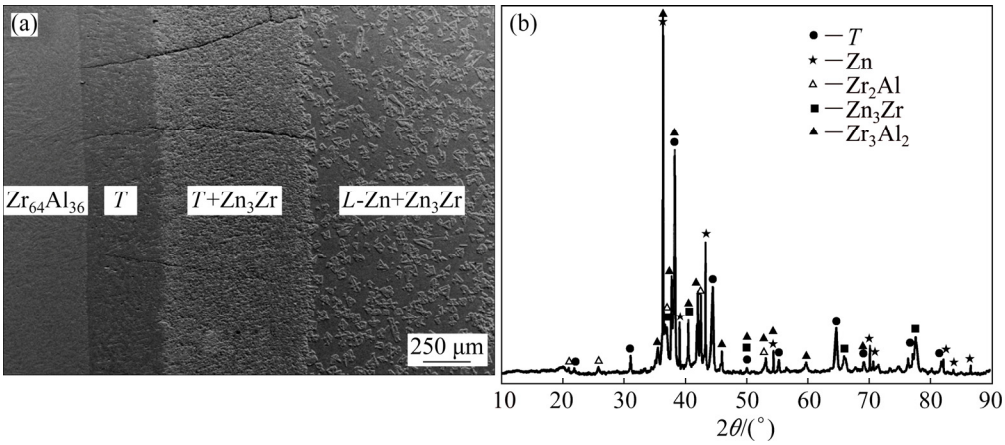

Fig. 1 Microstructure (a) and XRD pattern (b) of DC $Zr_{64}Al_{36}$/Zn annealed at 800 °C for 6 h

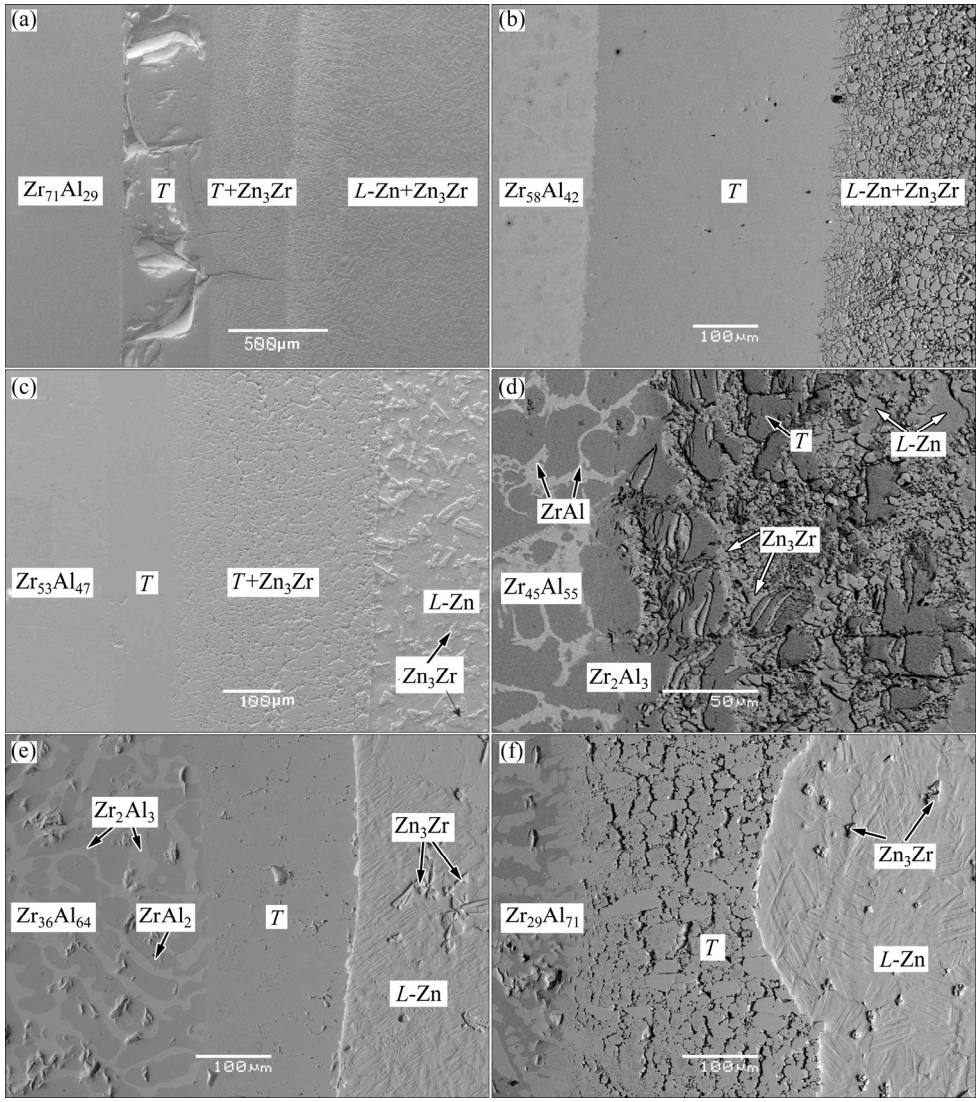

Fig. 2 Microstructures of DCs annealed at 800 °C for 6 h: (a) $Zr_{71}Al_{29}$/Zn; (b) $Zr_{58}Al_{42}$/Zn; (c) $Zr_{53}Al_{47}$/Zn; (d) $Zr_{45}Al_{55}$/Zn; (e) $Zr_{36}Al_{64}$/Zn; (f) $Zr_{29}Al_{71}$/Zn

The ternary compound *T* phase is in equilibrium with all the Al−Zr compounds at 800 °C, and it has a very large composition range of Al from 18.02 to 55.74 at.%, Zn from 16.84 to 54.35 at.% and Zr from 26.18 to 28.55 at.%. The maximum solubilities of Zn in $ZrAl_3$, $ZrAl_2$, ZrAl, Zr_2Al_3, Zr_4Al_3, Zr_3Al_2, Zr_2Al and Zr_3Al are 0.24, 0.64, 1.12, 0.91, 0.89, 0.33, 0.84 and 1.55 at.% (measured by EPMA), respectively.

3.2 Equilibrated samples

In order to investigate the phase equilibria of the Zn-rich and Al-rich corner of the Al−Zn−Zr system at 800 °C, a series of equilibrated samples on Al−Zn and Zn−Zr side were prepared. The nominal compositions of these typical alloys and all phases found in the equilibrium alloys are listed in Table 3. The composition of each phase represents the average composition of at least five measurements determined by EDS. The phases in each sample can be identified easily by their different morphology and chemical composition by SEM−EDS. Furthermore, the constituent phases were further identified by their X-ray diffraction patterns.

The three-phase equilibrium states of the *L*+*T*+$ZrAl_3$, *L*+Zn_3Zr+*T*, Zn_2Zr+*T*+Zn_3Zr, ZnZr+*T*+Zn_2Zr, ZnZr+*T*+Zr_3Al and Zr_3Al+ZnZr+*α*-Zr were experimentally determined by alloys A1−A6 using equilibrated alloy method. The typical microstructures and XRD patterns corresponding to the three-phase equilibrated states are shown in Fig. 3 (A1−A3) and Fig. 4 (A4−A6). From Fig. 3, it can be seen that alloys A1, A2 and A3 contain the large gray blocky *T* phase simultaneously. The ternary compound *T* phase has a large composition range of Al from 18.2 to 56.3 at.%, Zn from 17.2 to 55.1 at.% and Zr from 26.5 to 27.0 at.%. The result is similar to that determined by the diffusion couple method. Figure 3(a) shows the microstructure of alloy A1, and SEM−EDS analyses indicate that three phases, i.e., the black gray *L* phase, the gray blocky *T* and the light gray blocky $ZrAl_3$ phase, are equilibrated in the alloy. The typical XRD patterns of the three phases are shown in Fig. 3(b). The microstructure of alloy A2 is shown in Fig. 3(c) with the following three phases, i.e., the concave *L* phase, the small gray blocky Zn_3Zr phase and the large gray blocky *T* phase. The XRD pattern of alloy A2 shown in Fig. 3(d) confirms that the alloy locates in the *L*+*T*+Zn_3Zr field. As can be seen in Fig. 3(e), the microstructure of alloy A3 corresponds to Zn_3Zr+*T*+Zn_2Zr three-phase state. And also, three phases Zn_3Zr, *T* and Zn_2Zr are confirmed by their typical XRD patterns, as shown in Fig. 3(f).

Alloys A4, A5 and A6, which are in the three-phase equilibration regions, contain the ZnZr phase simultaneously. The microstructure and XRD pattern of alloy A4 are shown in Figs. 4(a) and (b), which indicates that the alloy corresponds to the Zn_2Zr+*T*+ZnZr three-phase equilibrium state. Figure 4(c) shows the microstructure of alloy A5, which indicates that the alloy is located in the *T*+ZnZr+Zr_3Al field. And Fig. 4(e) shows the microstructure of alloy A6. SEM−EDS analyses indicate that the black gray matrix is ZnZr phase, the light gray matrix is Zr_3Al phase and the gray grain is *α*-Zr phase. Experimental results listed in Table 3 indicate that the maximum solubilities of Zn in

Table 3 Compositions of alloys and phases in Al−Zn−Zr system at 800 °C (at.%)

Typical alloy	Designed composition	Phase	Composition/at.%		
			Zn	Al	Zr
A1	70Al−10Zn−20Zr	*T*	17.2	56.3	26.5
		L	10.4	89.5	0.1
		$ZrAl_3$	3.8	70.8	25.4
A2	10Al−70Zn−20Zr	*T*	55.1	18.4	26.5
		Zn_3Zr	72.9	1.5	25.6
		L	84.9	3.1	12.0
A3	10Al−60Zn−30Zr	*T*	54.8	18.2	27.0
		Zn_2Zr	67.8	1.3	30.9
		Zn_3Zr	72.9	1.6	25.5
A4	12Al−64Zn−24Zr	*T*	54.3	18.5	27.2
		Zn_2Zr	67.5	1.1	31.4
		ZnZr	37.1	13.2	49.7
A5	35Al−20Zn−45Zr	*T*	53.9	18.8	27.3
		Zr_3Al	5.4	19.7	74.9
		ZnZr	36.6	13.6	49.8
A6	25Al−20Zn−55Zr	*α*-Zr	0	3.6	96.4
		ZnZr	43.2	6.7	50.1
		Zr_3Al	7.5	17.3	75.2
A7	70Al−20Zn−10Zr	*T*	18.9	55.1	26.0
		L	20.9	78.9	0.2
A8	40Al−50Zn−10Zr	*T*	23.9	49.9	26.2
		L	62.6	35.2	2.2
A9	30Al−60Zn−10Zr	*T*	29.8	43.8	26.4
		L	70.1	25.3	4.6
A10	10Al−80Zn−10Zr	*T*	37.1	36.2	26.7
		L	81.5	8.2	10.3
A11	10Al−75Zn−15Zr	*T*	46.3	26.6	27.1
		L	83.7	4.5	11.8

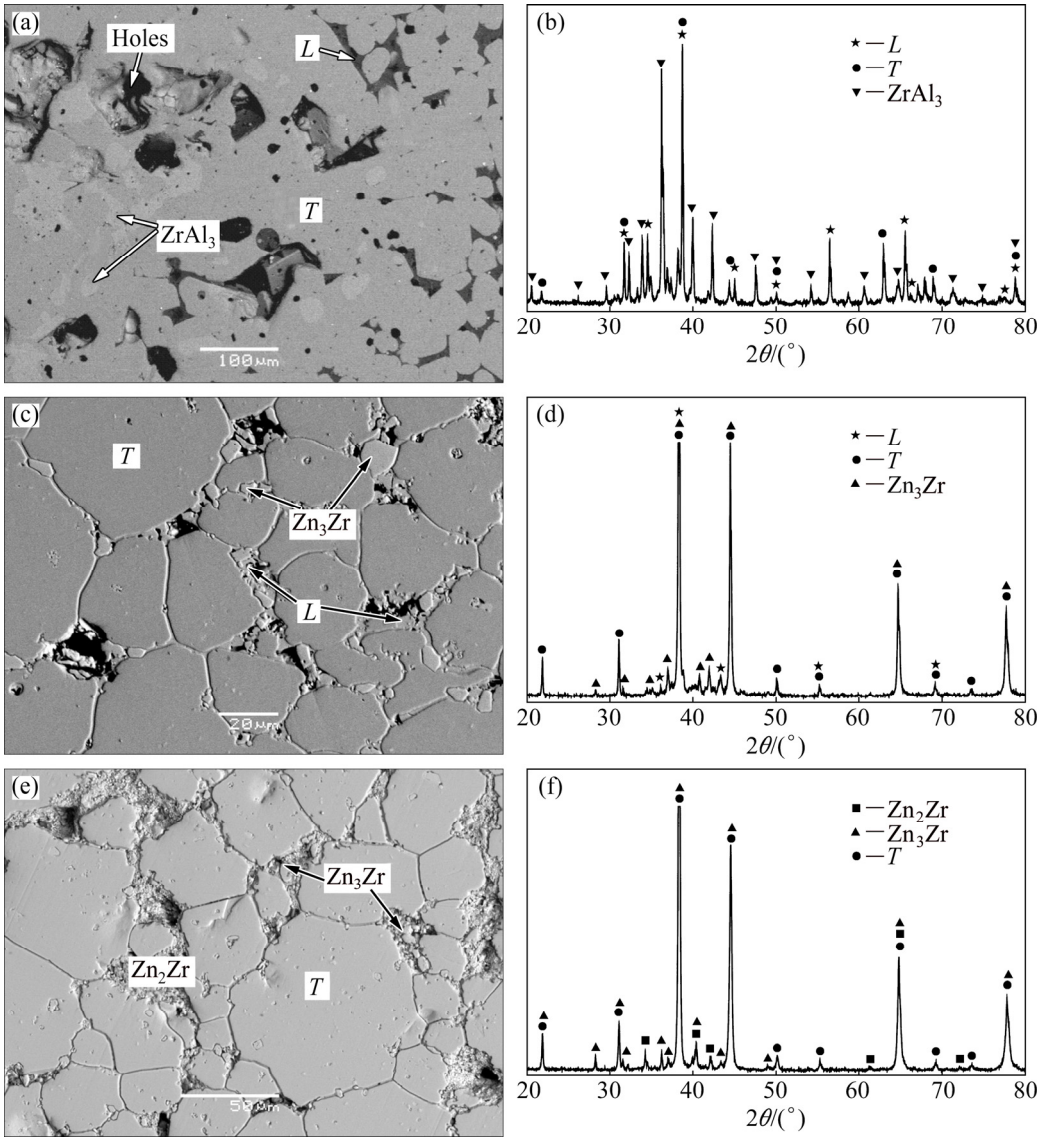

Fig. 3 Typical microstructures (a, c, e) and XRD patterns (b, d, f) corresponding to different three-phase fields of alloys A1−A3: (a, b) Alloy A1; (c, d) Alloy A2; (e, f) Alloy A3

$ZrAl_3$ and Zr_3Al are 3.8 and 7.5 at.%, and the maximum solubilities of Al in ZnZr, Zn_2Zr and Zn_3Zr are 13.6, 1.3 and 1.6 at.%, respectively.

Each of the alloys A7−A11 has two phases: *T*+*L*. These experimental results can be used to construct the boundary of liquid phase field near the Al−Zn side.

3.3 800 °C isothermal section of Al−Zn−Zr ternary system

Based on the information of three relevant binary systems [20,21,24] and the experimental results in the two different methods, the 800 °C isothermal section of the Al−Zn−Zr ternary system is constructed, as shown in Fig. 5(a). Thirteen three-phase regions in the isothermal section are confirmed by experiment. And the three-phase region ZnZr+*α*-Zr+*β*-Zr is inferred according to the contact rules of phase-region. The ternary compound *T* phase confirmed in the 450 °C isothermal section of Zn−Al−Zr ternary system [17] still exists at 800 °C. However, the composition range of *T* phase shrinks a little, from (11.9−58.5 at.% Zn, 15.7−61.8 at.% Al) to (16.84−55.1 at.% Zn, 18.02−56.3 at.% Al). Compared to Fig. 5(b), the phase relationship around *T* phase is different in the two isothermal sections. In the 450 °C isothermal section, the *T* phase is in equilibrium with *L*-Zn, *α*-Al, $ZrAl_3$, $ZrAl_2$, Zr_2Al_3, ZrAl, Zr_4Al_3, Zr_3Al_2, $Zn_{14}Zr$, Zn_6Zr and Zn_3Zr [16]. However, in the 800 °C isothermal section, the *T* phase equilibrates with almost all stable phases at this temperature, except for *α*-Zr and *β*-Zr. The three-phase region ZnZr+Zn_2Zr+ Zn_3Zr in the 450 °C isothermal section disappears at 800 °C. The maximum solubility of Al in Zn_2Zr and Zn_3Zr, of Zn in Zr_3Al decreases with the temperature increasing from 450 to 800 °C.

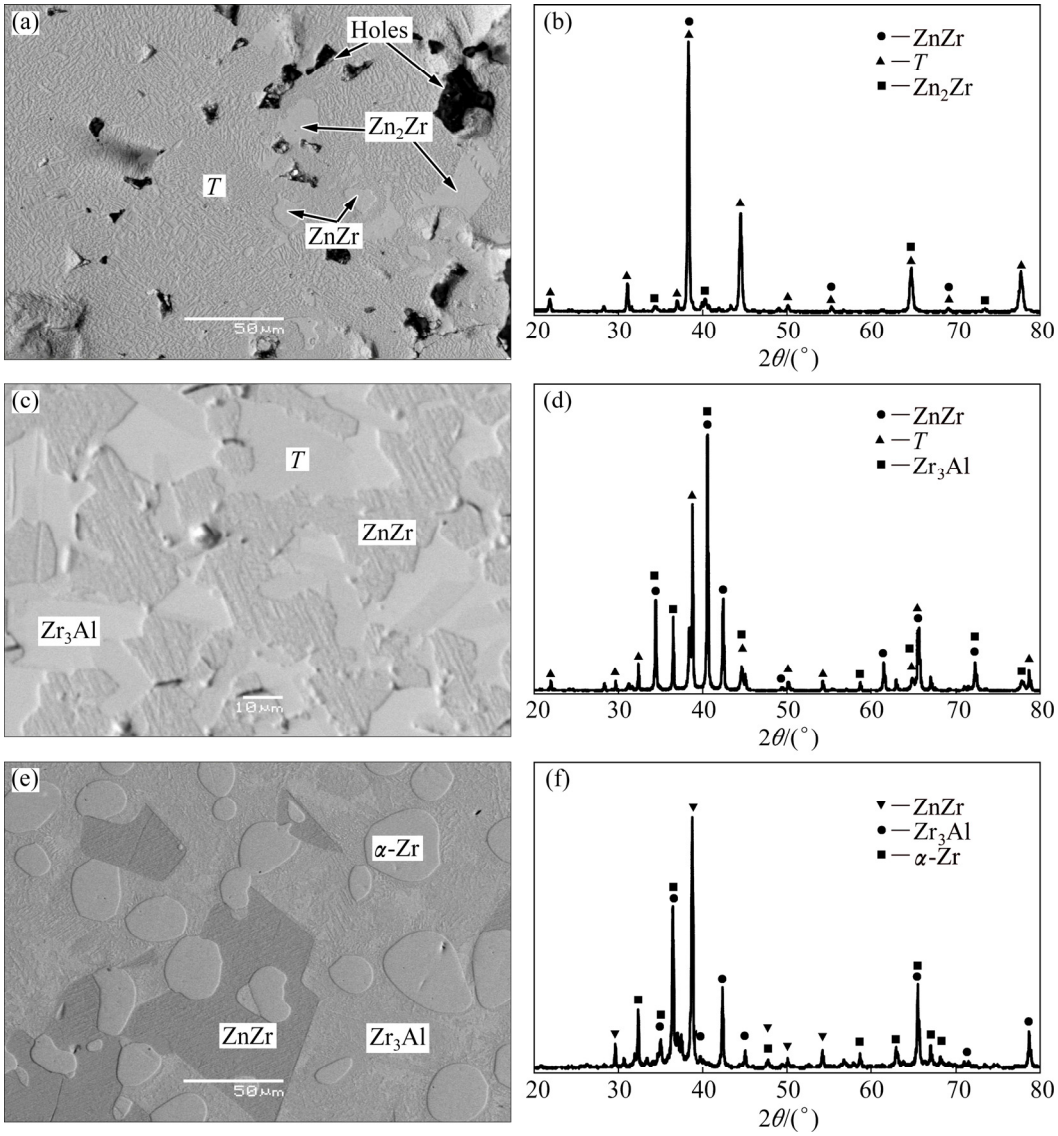

Fig. 4 Typical microstructures (a, c, e) and XRD patterns (b, d, f) corresponding to different three-phase fields of alloys A4−A6: (a, b) Alloy A4; (c, d) Alloy A5; (e, f) Alloy A6

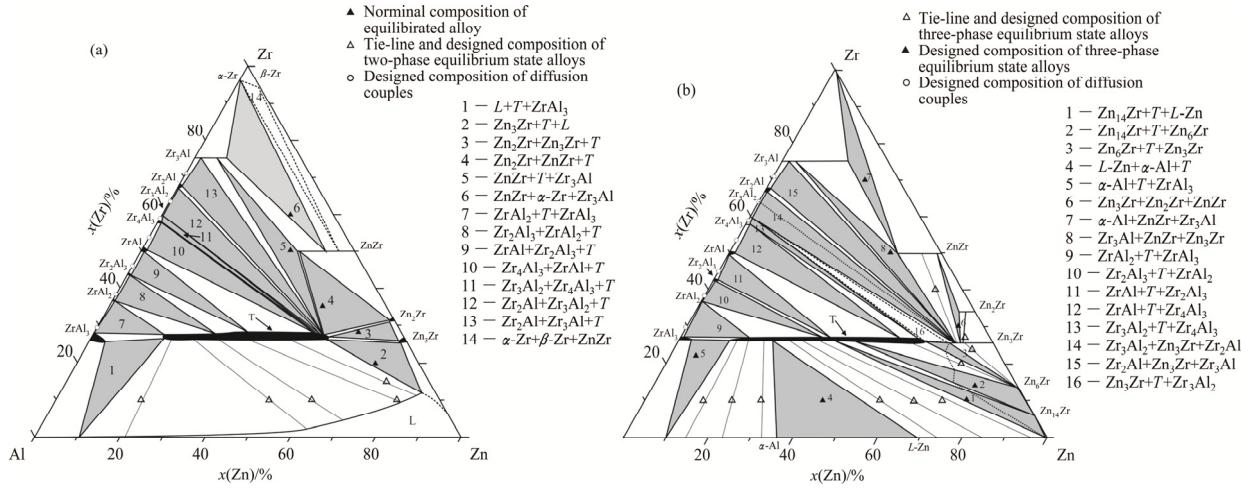

Fig. 5 Isothermal section of Al−Zn−Zr ternary system: (a) At 800 °C in this work; (b) At 450 °C [17]

4 Conclusions

(1) Thirteen three-phase regions are determined experimentally in the isothermal section of Al−Zn−Zr system at 800 °C.

(2) The ternary compound *T* is confirmed to be stable at 800 °C. It has a large composition range of Zn from 16.84 to 55.1 at.%. And it can be in equilibrium with all the binary compounds.

(3) The maximum solubilities of Zn in Zr_3Al, Zr_2Al, Zr_3Al_2, Zr_4Al_3, ZrAl, Zr_2Al_3, $ZrAl_2$ and $ZrAl_3$ are 7.5, 0.84, 0.33, 0.89, 0.91, 1.12, 0.64 and 3.8 at.%, respectively. The maximum solubilities of Al in Zn_3Zr, Zn_2Zr and ZnZr are 1.6, 1.3 and 13.6 at.%, respectively.

References

[1] HEINZ A, HASZLER A, KEIDEL C, MOLDENHAUER S, BENEDICTUS R, MILLER W S. Recent development in aluminium alloys for aerospace applications [J]. Materials Science and Engineering A, 2000, 280: 102−107.

[2] CHEN Lu, YAN An, LIU Hua-shan, LI Xiao-qian. Strength and fatigue fracture behavior of Al−Zn−Mg−Cu−Zr(−Sn) alloys [J]. Transactions of Nonferrous Metals Society of China, 2013, 23: 2817−2825.

[3] ZHANG Wei, XING Yuan, JIA Zhi-hong, YANG Xiao-fang, LIU Qing, ZHU Chang-luo. Effect of minor Sc and Zr addition on microstructure and properties of ultra-high strength aluminum alloy [J]. Transactions of Nonferrous Metals Society of China, 2014, 24: 3866−3871.

[4] WU H, WEN S P, GAO K Y, HUANG H, WANG W, NIE Z R. Effect of Er additions on the precipitation strengthening of Al−Hf alloys [J]. Scripta Materialia, 2014, 87: 5−8.

[5] DEV S, STUART A A, KUMAAR R C R D, MURTY B S, RAO K P. Effect of scandium additions on microstructure and mechanical properties of Al−Zn−Mg alloy welds [J]. Materials Science and Engineering A, 2007, 467: 132−138.

[6] SUN Y W, JOHNSON D R, TRUMBLE K P. Effect of Zr on recrystallization in a directionally solidified AA7050 [J]. Materials Science and Engineering A, 2017, 700: 358−365.

[7] WU H, WEN S P, HUANG H, LI B L, WU X L, GAO K Y, WANG W, NIE Z R. Effects of homogenization on precipitation of Al_3(Er,Zr) particles and recrystallization behavior in a new type Al−Zn−Mg−Er−Zr alloy [J]. Materials Science and Engineering A, 2017, 689: 313−322.

[8] YIN Z M, YANG L, PAN Q L, JIANG F. Effect of minor Sc and Zr on the microstructure and mechanical properties of Al−Zn−Mg based alloys [J]. Transactions of Nonferrous Metals Society of China, 2001, 11: 822−825.

[9] WANG X, CHEN G Q, LI B, WU L M, JIANG D M. Effects of Sc, Zr and Ti on the microstructure and properties of Al alloys with high Mg content [J]. Rare Metals, 2010, 29(1): 66−71.

[10] JIAO L, ZHAO Y T, CHEN J C, CHEN L. Microstructure and properties of Al_3Zr/2024Al in situ composites after forging [J]. Rare Metals, 2016, 35(12): 920−925.

[11] LIU Bin, WANG Ming-pu, LEI Qian, DUAN Yu-lu, LIU Lin-xian, YU Hong-chun. Microstructure and properties of Al−Zn−Mg−Cu−Zr alloy prepared by spray deposition method [J]. Transactions of Nonferrous Metals Society of China, 2015, 25(7): 1773−1780.

[12] EIVANI A R, AHMED H, ZHOU J, DUSZCZYK J. An experimental and theoretical investigation of the formation of Zr-containing dispersoids in Al−4.5Zn−1Mg aluminum alloy [J]. Materials Science and Engineering A, 2010, 527(9): 2418−2430.

[13] ROBSON J D, PRANGNELL P B. Dispersoid precipitation and process modelling in zirconium containing commercial aluminium alloys [J]. Acta Materialia, 2001, 49(4): 599−613.

[14] MORERE B, MAURICE C, SHAHANI R, DRIVER J. The Influence of Al_3Zr dispersoids on the recrystallization of hot-deformed AA7010 alloys [J]. Metallurgical and Materials Transactions A, 2001, 32(3): 625−632.

[15] MARDER A R. The metallurgy of zinc-coated steel [J]. Progress in Materials Science, 2000, 45: 191−271.

[16] ZHANG B. Development of corrosion resistant galvanizing alloys (Birmingham) [D]. Birmingham: The University of Birmingham, 2005: 137−144.

[17] CHEN L P, YIN F C, OUYANG X M, ZHAO M X. Experimental investigation of the phase equilibria of the Zn−Al−Zr ternary system at 723 K (450 °C) [J]. Metallurgical and Materials Transactions A, 2015, 46(11): 4956−4965.

[18] MEY S A. Reevaluation of the Al−Zn system [J]. International Journal of Materials Research, 1993, 84: 451−455.

[19] CHEN S L, CHANG Y A. A Thermodynamic analyses of the Al−Zn system and phase diagram calculation [J]. Calphad, 1993, 17: 113−124.

[20] MASSALSKI T B, OKAMOTO H, SUBRAMANIAN P R, KACPRZAK L. Binary alloy phase diagrams [M]. 2nd ed. Materials Park: ASM, 1990.

[21] DUTKIEWICZ J. The Zn−Zr (zinc-zirconium) system [J]. Journal of Phase Equilibria and Diffusion, 1992, 13(4): 430−433.

[22] WILLIAMS M E, BOETTINGER W J, KATNER U R. Contribution to the Zr-rich part of the Zn−Zr phase diagram [J]. Journal of Phase Equilibria and Diffusion, 2004, 25(4): 355−363.

[23] ARROYAVE R, LIU Z K. Thermodynamic modelling of the Zn−Zr system [J]. Calphad, 2006, 30(1): 1−13.

[24] OKAMOTO H. Al−Zr (aluminum-zirconium) [J]. Journal of Phase Equilibria and Diffusion, 1993, 14: 259−260.

[25] WANG T, JIN Z P, ZHAO J C. Thermodynamic assessment of the Al−Zr binary system [J]. Journal of Phase Equilibria and Diffusion, 2001, 22: 544−551.

[26] DRASNER A, BLAZINA Z. Structural studies in the systems $ZrZn_{2-x}Al_x$ and $HfZn_{2-x}Al_x$ [J]. Zeitschrift fur Naturforschung Section A, 1981, 36b: 1547−1550.

[27] SCHUBERT K, MEISSNER H G, RAMAN A, ROSSTEUTSCHER W. Some structural information of metallic phases (9) [J]. Naturwissenschaften, 1964, 51: 287.

[28] CLARK N J, WU E. Hydrogen absorption in the Zr−Al system [J]. Journal of the Less Common Metals, 1990, 163: 227−243.

[29] MURRAY J, PERUZZI A, BARILOCHE J P. The Al−Zr (aluminum−zirconium) system [J]. Journal of Phase Equilibria and Diffusion, 1992, 13: 277−291.

[30] HAFEZ M, SLEBARSKI A. Magnetic and structural investigations of $Zr_{1-x}Gd_xAl_2$ alloys [J]. Journal of Magnetism and Magnetic Materials, 1990, 89: 124−128.

[31] MA Y, ROMMING C, LEBECH B, GJONNES J, TAFTO J. Structure refinement of Al_3Zr using single-crystal X-ray diffraction, powder neutron diffraction and CBED [J]. Acta Crystallographica Section B, 1992, 48: 11−16.

[32] VILLARS P, CALVERT L D. Pearson's handbook of crystallographic data for intermetallic phases [M]. 4 ed. Materials Park, ASM International, 1991: 53−65.

[33] SCHREURS L W M, WEIJERS H M, DEURSEN A P J, VROOMEN A R. Growth and electrical properties of $ZrZn_2$ single crystals [J]. Materials Research Bulletin, 1989, 24: 1141−1145.

[34] SU X P, TANG N Y, TOGURI J M. 450 °C isothermal section of the Fe−Zn−Si ternary phase diagram [J]. Canadian Metallurgical Quarterly, 2001, 40: 337−384.

[35] GUO Z K, LIN Z X, YAN T S. High temperature phase equilibria and phase diagrams [M]. Shanghai: Shanghai Scientific and Technical Publishers, 1987. (in Chinese)

Al−Zn−Zr 三元系 800 °C 等温截面的实验测定

刘永雄[1,2]，尹付成[1,2]，李 智[1,2]，欧阳雪枚[1,2]，陈亮平[1,2]

1. 湘潭大学 材料科学与工程学院，湘潭 411105；
2. 湘潭大学 材料设计及制备技术湖南省重点实验室，湘潭 411105

摘 要：利用扩散偶和平衡合金法，采用扫描电镜−能谱、X 射线衍射和电子探针分析方法对 Al−Zn−Zr 三元系 800℃等温截面进行实验测定。实验确定了 13 个三相区；三元化合物 $Zn_{50}Al_{25}Zr_{25}$(*T* 相)稳定存在于此等温截面，拥有比较大的成分区间(16.84%~55.1% Zn、18.02%~56.3% Al 和 26.0%~28.53% Zr，摩尔分数)，并能与该体系中所有的二元化合物平衡共存。Zn 在 Zr−Al 化合物 Zr_3Al、Zr_2Al、Zr_3Al_2、Zr_4Al_3、ZrAl、$ZrAl_2$、$ZrAl_3$、$ZrAl_2$ 和 $ZrAl_3$ 中最大溶解度分别是 7.5%、0.84%、0.33%、0. 89%、0.91%、1.12%、0.64%和 3.8%(摩尔分数)；Al 在 Zn−Zr 化合物 Zn_3Zr、Zn_2Zr 和 ZnZr 中最大溶解度分别是 1.6%、1.3%和 13.6%(摩尔分数)。

关键词：Al−Zn−Zr 三元系；相图；$Zn_{50}Al_{25}Zr_{25}$；SEM−EDS；EPMA

(Edited by Bing YANG)